Acta Biomaterialia

Iontophoresis-Driven Porous Microneedle Array Patch for Active Transdermal Drug Delivery

--Manuscript Draft--

Manuscript Number:	AB-20-2127
Article Type:	Full length article
Section/Category:	Opt in to First Look
Keywords:	Transdermal drug delivery; Porous microneedle array; Iontophoresis; Skin penetration; Diabetes
Abstract:	Transdermal patch combined microneedle array (MA) with iontophoresis can achieve synergistic and remarkable enhancement for drug delivery with precise electronic control. However, development of a MA patch combined with iontophoresis, that is in situ treatment, easy self-administration, and controllable delivery of liquid macromolecular drugs, is still a challenge. Here, we presented a novel iontophoresis-driven porous MA patch (IDPMAP) for in situ, patient-friendly, and active delivery of charged macromolecular drugs. IDPMAP integrates porous MA with iontophoresis into a single transdermal patch, realizing one-step drug administration strategy of “Penetration, Diffusion and Iontophoresis”. Moreover, a matching portable iontophoresis-driven device was developed for drug self-administration of IDPMAP. In vitro and in vivo studies showed that IDPMAP had excellent skin penetration ability, negligible cytotoxicity and good biocompatibility without skin irritation and hypersensitivity. In vivo transdermal insulin delivery in type-1 diabetic rats demonstrated that IDPMAP could effectively deliver insulin nanovesciles and produce robust hypoglycemic effect on diabetic rats, with more advanced controllability and efficiency compared with pristine MA or iontophoresis. IDPMAP and its portable iontophoresis-driven device are user-friendly that shows a promising potential for drug self-administration at home.

Powered by Editorial Manager® and ProduXion Manager® from Aries Systems Corporation
Electronic copy available at: https://ssrn.com/abstract=3677349

Statement of Significance

Transdermal patch combined microneedle array (MA) with iontophoresis has a synergistic enhancement in drug delivery. However, it is still a challenge to develop a MA patch coupled with iontophoresis, that is in-situ treatment, easy self-administration, and active delivery of macromolecular drugs. Herein, we developed a novel iontophoresis-driven porous MA patch (IDPMAP) and portable iontophoresis-driven device for active transdermal delivery of charged liquid drugs. IDPMAP integrates porous MA and iontophoresis into a single patch, realizing one-step drug administration approach of "Penetration, Diffusion and Iontophoresis". IDPMAP had robust drug delivery ability with more advanced controllability and efficiency compared with pristine MA or iontophoresis. Above all, IDPMAP and iontophoresis-driven device offers a platform technique for effective drug delivery in an active-controlled manner.

Electronic copy available at: https://ssrn.com/abstract=3677349

Graphical Abstract

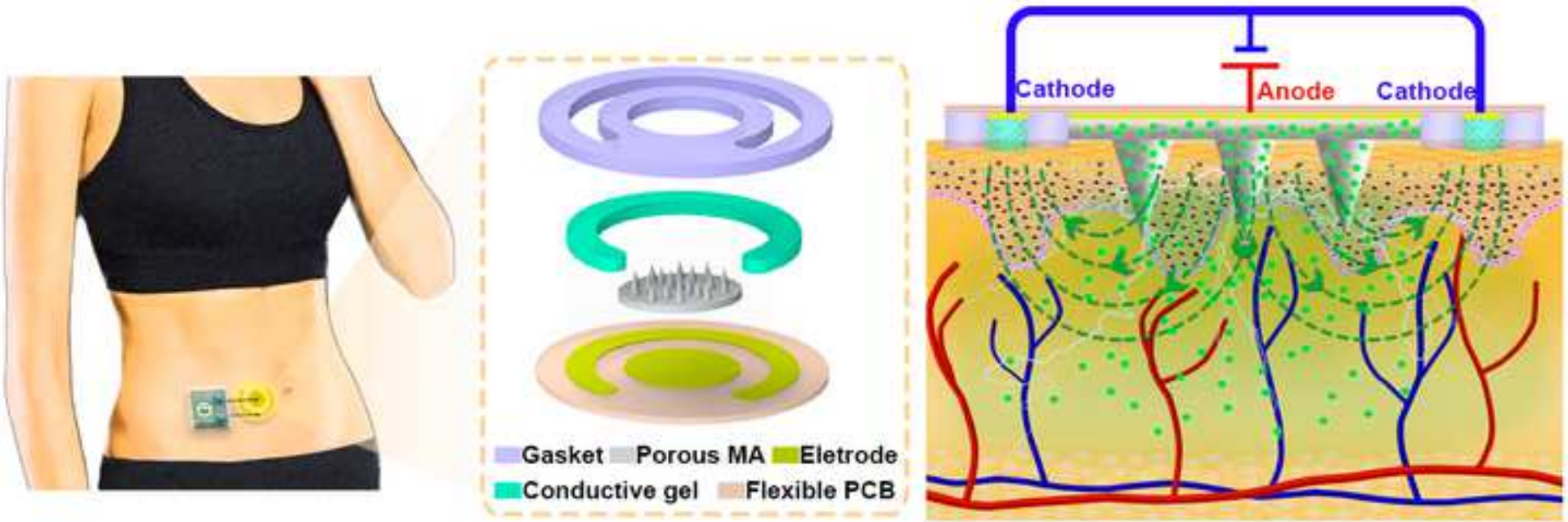

Electronic copy available at: https://ssrn.com/abstract=3677349

Manuscript File

Click here to view linked References

Iontophoresis-Driven Porous Microneedle Array Patch for Active Transdermal Drug Delivery

Yanjun Li[1], Jingbo Yang[1], Rui Ye[1], Bin Liu[1], Yong Huang[3], Wei Zhou*[,2], Lelun Jiang*[,1]

1. Guangdong Provincial Key Laboratory of Sensor Technology and Biomedical Instrument, School of Biomedical Engineering, Sun Yat-sen University, Guangzhou, PR China;

2. Department of Mechanical and Electrical Engineering, Xiamen University, Xiamen, PR China;

3. Guangdong Medical Devices Quality Surveillance and Test Institute, Guangzhou, PR China;

* Corresponding authors, E-mail: jianglel@mail.sysu.edu.cn; weizhou@xmu.edu.cn

ABSTRACT

Transdermal patch combined microneedle array (MA) with iontophoresis can achieve synergistic and remarkable enhancement for drug delivery with precise electronic control. However, development of a MA patch combined with iontophoresis, that is in situ treatment, easy self-administration, and controllable delivery of liquid macromolecular drugs, is still a challenge. Here, we presented a novel iontophoresis-driven porous MA patch (IDPMAP) for in situ, patient-friendly, and active delivery of charged macromolecular drugs. IDPMAP integrates porous MA with iontophoresis into a single transdermal patch, realizing one-step drug administration strategy of "Penetration, Diffusion and Iontophoresis". Moreover, a matching portable iontophoresis-driven device was developed for drug self-administration of IDPMAP. *In vitro* and *in vivo* studies showed that IDPMAP had excellent skin penetration ability, negligible cytotoxicity and good biocompatibility without skin irritation and hypersensitivity. *In vivo* transdermal insulin delivery in type-1 diabetic rats demonstrated that IDPMAP could effectively deliver insulin nanovesciles and produce robust hypoglycemic effect on diabetic rats, with more advanced controllability and efficiency compared with pristine MA or iontophoresis. IDPMAP and its portable iontophoresis-driven device are user-friendly that shows a promising potential for drug self-administration at home.

Keywords: Transdermal drug delivery; Porous microneedle array; Iontophoresis; Skin penetration; Diabetes

1. INTRODUCTION

Transdermal drug delivery system has a variety of potential advantages over other routes of drug administration [1-3]. It could avoid hepatic first-pass metabolism associated with oral delivery and is less painful than injections [3, 4]. However, the outmost layer of skin, the stratum corneum, poses a barrier to the entry of many therapeutic entities into the systemic circulation, particularly high molecular weight drugs [1, 2]. Therefore, approaches for skin permeability enhancement are needed to overcome the stratum corneum barrier layer and improve transdermal permeation rate of macromolecular drugs across the skin [3, 4].

Microneedle array (MA) has been considered as one of the most promising transdermal drug delivery system owing to its unique advantages of pain-free delivery, minimal skin trauma, lack of bleeding, self-administration, and ease of disposal [5-9]. However, MA-based delivery typically relies on relatively slow drug diffusion through MA-induced micro-holes in the skin or dissolution of drug-loaded MA or drug coatings on MA [8, 10-12]. Thus, MA is in stark contrast to the rapid delivery of liquid drug formulations with a large dosage using the conventional subcutaneous injection. Iontophoresis uses a mild electric current to safely drive charged drugs or uncharged compounds across

Electronic copy available at: https://ssrn.com/abstract=3677349

the stratum corneum through electrophoresis and electroosmotic flow [3, 13-17]. The combination of skin barrier impairment using MA coupled with iontophoresis has demonstrated a synergistic enhancement in transdermal delivery with the added benefit of precise electronic control [18-20]. It also may enable bolus, pulsatile or responsive drug administration [19, 21]. Therefore, MA coupled with iontophoresis is a promising transdermal drug administration strategy.

Solid MA, hollow MA, or swelling MA coupled with iontophoresis using corresponding drug administration approaches have been reported [18, 22, 23]. The drug administration strategy of solid MA with iontophoresis is "poke and removal, and iontophoresis". Solid MA combined with iontophoresis can actively deliver charged macromolecule drugs [18, 24]. However, it required two-step for transdermal drug delivery (poke and removal using solid MA, then iontophoresis patch applied), resulting in practicality issues for patients. Furthermore, the created micro-holes in the skin would gradually shrink and self-heal within a short period after removal of solid MA, which dramatically limits the available administration period [23, 25]. Hollow MA coupled with iontophoresis can one-step drive the charged drugs through the central bore of hollow MA into systematic circulation by electric stimulus [22]. However, the bore of hollow MA may be blocked by compressed dermal tissue during MA insertion [10]. Recently, the amalgamation of iontophoresis with hydrogel swelling MA was developed for in situ macromolecule drug delivery [23]. However, the poked hydrogel MA should firstly absorb interstitial fluid from skin to realize MA swelling and thereby form the interconnecting channels for iontophoresis of charged drugs, resulting in a slow drug release rate at initial stage. Moreover, the cross-linking process for preparation of hydrogel MA may lead to inactivation of drugs [25]. Above all, development of a transdermal patch combined MA with iontophoresis, that is in situ treatment, easy self-administration, active and long-term delivery of liquid macromolecular drugs, is still a challenge.

Herein, we developed a novel iontophoresis-driven porous MA patch (IDPMAP) for in situ, patient-friend, and long-lasting transdermal delivery of a wide range of liquid macromolecular drugs, as shown in Figure 1. This IDPMAP well integrates porous MA with iontophoresis into a single transdermal patch, achieving one-step drug administration approach of "Penetration, Diffusion and Iontophoresis". Porous MA of IDPMAP utilized its interconnecting pores for storage and iontophoresis-driven delivery of charged liquid drugs. Furthermore, we developed an embedded microcontroller-based iontophoresis-driven device for active drug administration of IDPMAP. To our knowledge, there have been no report on IDPMAP and portable iontophoresis-driven device for transdermal drug delivery.

2. EXPERIMENTAL SECTION

2.1 Ethics statement

All animal procedures conducted in this work were reviewed, approved, and supervised by the Institutional Animal Care and Use Committee at the Sun Yat-Sen University (Approval Number: IACUC–DD–16–0904).

2.2 Materials and animals

Polydimethylsiloxane (PDMS, Sylgard 184) was purchased from Dow Corning, England. For fabrication of porous MA, polyethylene glycol (PEG), 2-methoxyethanol, glycidyl methacrylate, trimethylolpropane trimethacrylate (TRIM), and triethylene glycol dimethacrylate (TEGDMA) were obtained from Macklin, China. Dulbecco's Modified Eagle's Medium (Gibco, Invitrogen), fetal bovine

Electronic copy available at: https://ssrn.com/abstract=3677349

serum (Gibco, USA) and penicillin–streptomycin (Gibco, USA) were bought for cell culture. 3-(4,5-dimethylthiazol-2-yl)-2,5-diphenyltetrazolium bromide (Sigma, USA), dimethyl sulfoxide (Sigma, USA) and Calcein-AM/PI kit (BestBio, China) were purchased for cytotoxicity test of IDPMAP. Bovine insulin (27 IU/mg, CAS: 11070-73-8, China), soybean lecithin (Tianjin Chemical Reagent Co. Ltd, China), propylene glycol (Tianjin Chemical Reagent Co. Ltd, China) and cetyltrimethyl ammonium bromide (Shanghai Aobo Chemical Reagent Co. Ltd, China) were purchased for preparation of insulin nanovesicles. Streptozotocin (Sigma, USA) was bought to induce type-1 diabetes in Sprague-Dawley rats.

The insulin nanovesicles solution was prepared by ultrasonic dispersion method [18]. Bovine insulin (27 IU/mg) was firstly dissolved in Tris-HCl (pH 7.0, 0.5 M), then titrated HCl (1 M) till transparent, tuned pH at 7.4 using NaOH (0.5 M), and finally obtained insulin stock solution at a proper concentration by adding phosphate-buffered saline (PBS, pH 7.4). Subsequently, soybean lecithin (1.5 g) dissolved in propylene glycol (3 g) was uniformly mixed into the insulin stock solution (94.5 g) by ultrasonic (800 W, 1:1) for 40 min. Next, cetyltrimethyl ammonium bromide (4 wt%) was added to the mixture and gently shaken to obtain positively charged insulin nanovesicles. The morphology of insulin nanovesicles was observed using the transmission electron microscopy (TEM, JEOL-2100F, Japan). The average diameters, zeta potentials and polydispersity index of nanovesicles were measured using a photon correlation spectroscopy (Nano ZS90, Malvern Instruments, U.K).

Fresh rabbit skin was prepared for mechanical test. A New Zealand rabbit (male, 2-3 months old, and 3.0 kg) was purchased from the Xinhua Experimental Animal Farm (Guangzhou, China). Fresh rabbit skin for mechanical test was prepared by shaving hair and removal of subcutaneous fat. Sprague–Dawley rats (male, 200 ± 30 g) for *in vivo* transdermal insulin delivery were provided by the Experimental Animal Center of Sun Yat-sen University, China. NIH/3T3 mouse fibroblast for cytotoxicity test was bought from Xiangbo Biotechnology Co., Ltd, China. The first three generations of passage at 60 % confluency were used in cytotoxicity study.

2.3 Fabrication of IDPMAP

The fabrication process of porous MA is: (1) Preparation of stock solution for porous MA: PEG (0.55g) was dissolved into 2-methoxyethanol (2.75 ml) at 50 ℃as a porogen stock solution. Subsequently, the monomer GMA (1 ml; 2.75 mmol, 1 equiv.), crosslinker TRIM (0.68 ml; 1.94 mmol, 0.26 equiv.), and crosslinker TEGDMA (1.59 ml; 5.76 mmol, 0.79 equiv.) were uniformly mixed as a monomer stock solution. Next, a photoinitiator Irgacure 184 (0.10 g, 1 wt% to the monomer) was added into the mixture of the monomer and porogen stock solutions. (2) Preparation of female mold: an aluminum MA was firstly fabricated by micromachining technique. It consists of 138 conical microneedles with a height of approximately 800 μm, base diameter of approximately 400 μm, and distance between two adjacent microneedles of 1 mm. A female PDMS mold with hole array was fabricated using the aluminum MA by typical micro-molding technique [26]. (3) Fabrication of porous MA [27, 28] (Figure S1). Briefly, the prepared stock solution was casted in the female PDMS mold under a vacuum of approximately 2000 Pa. MA was solidified in the PDMS mold by ultraviolet irradiation (INTELLI-RAY 400, Uvitron, USA) for 15 min and peeled off from PDMS mold. The solid MA was immersed in 75 % ethanol solution for 24 h to remove the porogen of PEG. The porous MA was fabricated and its morphology was observed using

Electronic copy available at: https://ssrn.com/abstract=3677349

a scanning electron microscope (SEM, Quanta 400F, Oxford, Holland).

IDPMAP was assembled with a porous MA, an anti-seepage gasket, a conductive hydrogel, and two Ag/AgCl electrodes on flexible PCB, as shown in Figure 1a. The porous MAs were sterilized by high pressure steam for 30 min before use. Ag/AgCl ink (Bioelectro Analytical Science Inc, Japan) was printed on flexible PCB to prepare the Ag/AgCl electrodes. The anti-seepage gasket was cut from 3M medical tape by focused laser beam. The agarose hydrogel (2 % w/v) containing normal saline was used for conductive gel.

2.4 Design of iontophoresis-driven device

An iontophoresis-driven device was developed for regulation of output iontophoresis current. A miniature iontophoresis-driven PCB (size: 38×32×2 mm^3) based on ultralow power microcontroller of MSP430F169 (Texas Instruments, USA) was designed and fabricated, as shown in Figure S2 and Figuer S3 of *Supporting Information*. The circuit schematic diagram of the iontophoresis-driven PCB was designed by Altium Designer (Altium, Australia). An self-developed program based on C language was compiled and burned in MSP430F169. The insulation shell (44× 38 ×10 mm^3) of iontophoresis-driven device was 3D printed (Sindon, 3DWOX, Korea) for electrical safety, as shown in Figure 2a.

2.5 Mechanical tests of IDPMAP

The mechancial tests of IDPMAP were performed using a universal testing machine (5543A, Instron, USA). Fracture performance of IDPMAP was firstly tested, as shown in Figure S4a. An IDPMAP was perpendicularly compressed by an Al plate at a speed of 0.1 mm/s. The compression stopped till the loading force reached 10 N [29]. The loading force and displacement were simultaneously recorded. The fractured porous MA was observed using SEM. *In vitro* skin penetration of IDPMAP was also tested, as shown in Figure S4b. A fresh rabbit skin was firstly fixed on a polystyrene foam [30]. Microneedle tips of IDPMAP were loaded with a red tissue-marking dye [31]. IDPMAP attached on upper Al plate was pressed toward rabbit skin at a speed of 0.1 mm/s till the loading force reached 10 N. The loading force and displacement were recorded. The rabbit skin and the porous MA after skin penetration were also observed using SEM and an optical microscope. The poked skin was immediately soaked in a tissue fixation solution (4% paraformaldehyde) overnight at 4 ℃ and subsequently observed by optical coherence tomography (OCT). The penetration ratio was calculated by dividing the number of poked pores with red dots by the microneedle number of porous MA [32].

2.6 Cytotoxicity study of porous MA

Porous MA, the key component of IDPMAP, is penetrated in the skin to deliver drugs. Thus, cytotoxicity study toward porous MA was performed using NIH/3T3 fibroblasts [33]. Cells were cultured in Dulbecco's Modified Eagle's Medium with 10 % (v/v) fetal bovine serum and 1 % penicillin–streptomycin. The sterilized porous MAs were immersed in the cell culture medium at a concentration of 0.2 g/ml, and incubated at 37 ℃ for 24 h. Finally, a releasing media of porous MA was obtained. Cell viability was measured by 3-(4,5-dimethylthiazol-2-yl)-2,5-diphenyl tetrazolium bromide (MTT) assay. Briefly, cells were seeded in 96-well plates with a density of 3,000 cells per well and cultured overnight. The original culture medium was replaced by 100 µl releasing media per well. After 48 h incubation, the cells were washed with PBS solution and incubated by addition of 20 µL MTT solution (5 mg/mL) and 100 µL fresh culture medium for 4 h. Next, the original solution was replaced by 150 µL dimethyl

Electronic copy available at: https://ssrn.com/abstract=3677349

sulfoxide, and the plates was incubated at 37 ℃ for 15 min. The absorbance of the plates was measured using microplate reader (Infinite M200 Pro, Tecan, Morrisville, NC, USA).

The cells incubated with the releasing media were stained with a Calcein-AM/PI kit. Cells were seeded in 6-well plates at a density of 20,000 per well and cultured overnight. The releasing media was added to the plates to incubate the cells with 2 ml per well for 48 h. According to the manufacturer's instructions, Calcein-AM/PI were added in each well [34, 35]. The pictures of stained cells were captured by the fluorescence microscope (Nikon ECLIPSE Ti, Japan). Calcein $\lambda_{ex/em}$: 485/535 nm, PI $\lambda_{ex/em}$: 530/620 nm.

2.7 *In vivo* transdermal insulin delivery

Type-1 diabetic rats were induced by injection of Streptozotocin (STZ) at a dose of 60 mg/kg [36]. The injected rats were fasted but drunk freely for one night. The blood glucose levels (BGLs) of rats were continuously monitored for 7 days, and the rats whose BGLs were stable and higher than 16.65 mmol/L were selected for drug administration [25, 36]. The blood samples were collected from tail vein of the rats to measure BGLs by Roche blood glucose meter (Accu-Chek Performa).

The dorsal hair of all rats was shaved off the day before drug administration. The rats were randomly divided into 7 groups, as listed in Table 1: (a) healthy group, healthy rats without any treatment , (b) control group, diabetic rats without any treatment, (c) subcutaneous injection group, diabetic rats injected with 5 IU insulin nanovesicles, (d) IDPMAP/0mA iontophoresis (ITP) group, diabetic rats treated by IDPMAP loaded with 5 IU insulin nanovesicles without iontophoresis. (e) IDPMAP/0.5mA ITP group, diabetic rats treated by IDPMAP loaded with 5 IU insulin nanovesicles for 12 h and 0.5 mA iontophoresis for first 6 h. (f) IDPMAP/1mA ITP group, diabetic rats treated by IDPMAP loaded with 5 IU insulin nanovesicles for 12 h and 1 mA iontophoresis for first 6 h. (g) IDPMAP/1mA ITP (1:1) group, diabetic rats treated by IDPMAP loaded with 5 IU insulin nanovesicles for 12 h and a square wave current of 1 mA (200 Hz,1:1) for first 6 h. BGLs of the rats were measured every hour by Roche blood glucose meter. During drug administration, 200 μL of tail vein blood was collected every 2 hours to determine the concentration of serum insulin in rats. The blood samples were stored at 4 ℃ overnight, and the supernatant samples were obtained by centrifugation and stored at -80 ℃ until assayed. Serum insulin concentrations were measured using the bovine insulin ELISA kit (MEIMIAN, China).

The lungs, livers, spleens, kidneys and hearts of diabetic rats in IDPMAP/1mA group and control group after insulin treatment for 12 h were harvested after sacrifice, embedded in paraffin, and stained with hematoxylin and eosin. These organ slices were observed using an optical microscope.

Table 1 Rats groups for *in vivo* transdermal insulin nanovesicles delivery

Group name	Rats	Loading drug	MA	Iontophoresis
Healthy	Healthy rats	-	-	-
Control	Diabetic rats	-	-	-
Subcutaneous injection	Diabetic rats	Insulin nanovesicles	-	-
IDPMAP/0mA ITP	Diabetic rats	Insulin nanovesicles	Porous MA	0 mA
IDPMAP/0.5mA ITP	Diabetic rats	Insulin nanovesicles	Porous MA	0.5 mA
IDPMAP/1mA ITP	Diabetic rats	Insulin nanovesicles	Porous MA	1mA
IDPMAP/1mA ITP (1:1)	Diabetic rats	Insulin nanovesicles	Porous MA	1mA (200Hz, 1:1)

Electronic copy available at: https://ssrn.com/abstract=3677349

2.8 Statistical analysis

All of the results presented in this study were mean ± SD., and the number of samples was not less than three. The statistical analysis was carried out using two-sided Student's t-test, and $p < 0.5$ was considered statistically significant.

3. RESULTS AND DISCUSSION

3.1 Drug delivery mechanism of IDPMAP

An iontophoresis-driven porous MA drug delivery system is proposed for active transdermal drug delivery (Figure 1a and Video S1). The drug delivery system consists of an IDPMAP and a portable iontophoresis-driven device. The schematic circuit diagram of iontophoresis-driven device is illustrated in Figure 1c. The iontophoresis-driven device is powered by a lithium battery, which can be recharged by USB port. A microcontroller of MSP430F169 outputs the pulse width modulation (PWM) wave to regulate the voltage-controlled constant current for the iontophoresis of liquid drugs. The expanded view of IDPMAP is presented in Figure 1b. IDPMAP is composed of an anti-seepage gasket, a conductive hydrogel, a porous MA, and two Ag/AgCl electrodes on flexible PCB, which are concentrically bonded together. The porous MA is used for liquid drug carrier and skin penetration. The porous MA loaded with liquid drug and conductive hydrogel were chosen as the anode and cathode of iontophoresis, respectively. Once the iontophoresis-driven device outputs an iontophoresis current, the liquid drug stored in porous MA is gradually delivered into the skin by passive diffusion and active iontophoresis.

The drug administration strategy of IDPMAP is "Penetration, Diffusion and Iontophoresis" (Figure 1d and Video S1). (1) Skin penetration by porous MA. IDPMAP loaded with liquid drug can be fixed on the skin owing to the stickiness of gasket. Since the IDPMAP is pressed, the porous MA will penetrate through the stratum corneum layer in the dermal layer. (2) Passive diffusion of liquid drug. According to Fick's first law of diffusion, the drug solution stored in porous MA will passively diffuse into the skin through the interconnecting micro-pores. The drug diffusion speed is mainly determined by the drug solution concentration. (3) Active iontophoresis of liquid drug. The porous MA filled with ionic liquid drug is a good conductor for drug iontophoresis. A mild electric current is charged between porous MA and conductive hydrogel to drive charged therapeutic molecules from micro-pores into systemic circulation by the predominant driving forces of electromigration and electroosmosis [37-39]. The iontophoretic drug flux is mainly determined by the drug ions size, molecule charged potential, output current density, and treatment duration [21, 40, 41]. The breakthrough of porous MA in the stratum corneum will lead to the creation of aqueous pathways with low electrical resistance, contributing to a synergistic enhancement of MA coupled with iontophoresis. Furthermore, iontophoresis combined with electropositive nanovesicles capsuled with liquid drug further enhances the penetration of drug-loaded nanovesicles owing to the active electromigration and electroosmosis [42]. Above all, the drug administration strategy of IDPMAP is a combination of passive diffusion and active iontophoresis of electropositive nanovesicles capsuled with liquid drug.

Electronic copy available at: https://ssrn.com/abstract=3677349

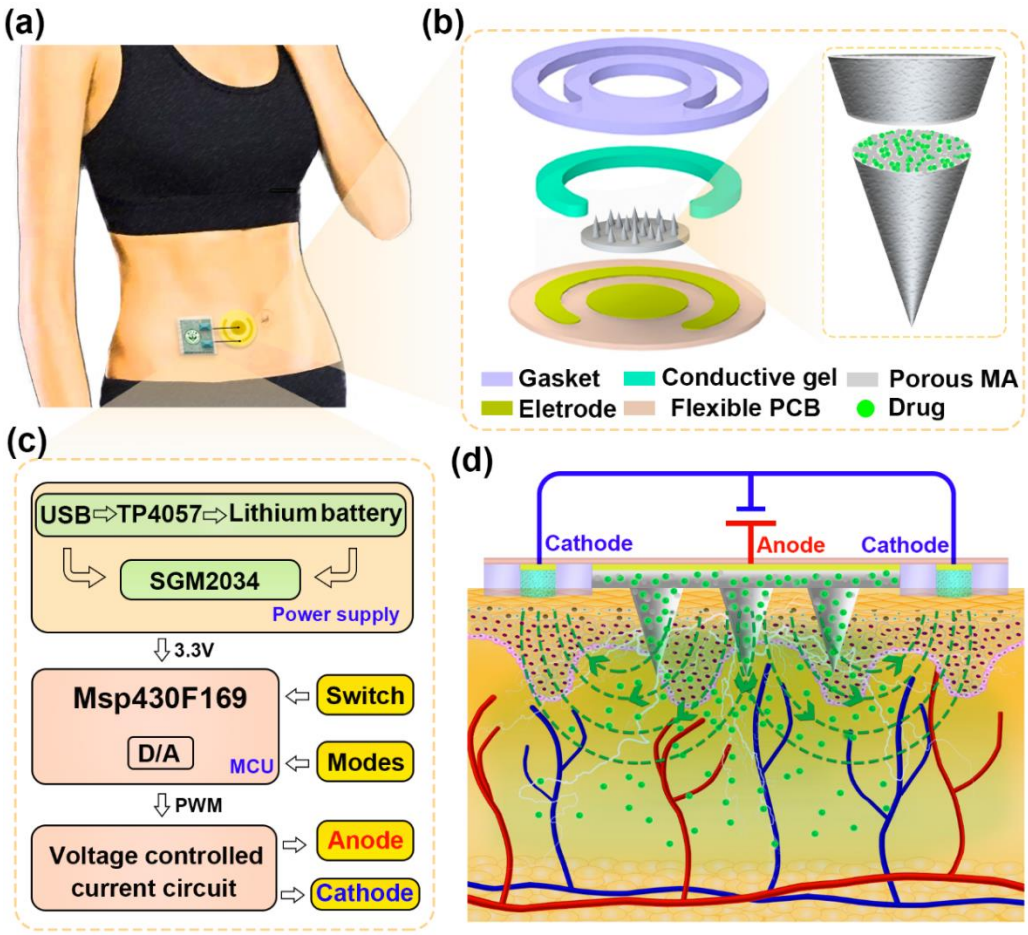

Figure 1 (a) Schematic illustration of the iontophoresis-driven porous MA drug delivery system. It mainly consists of an IDPMAP and a miniature iontophoresis-driven device. (b) Exploded view of IDPMAP. IDPMAP is composed of an anti-seepage gasket, a conductive hydrogel, a porous MA, and a pair of Ag/AgCl electrodes on flexible PCB. (c) Schematic circuit diagram of the iontophoresis-driven device. The iontophoresis-driven device is used to output the iontophoresis current for IDPMAP. (d) Schematic representation of the drug administration strategy of IDPMAP. Liquid drug stored in the pores of IDPMAP is released into the skin under the sum effect of active iontophoresis and passive diffusion.

3.2 Design and fabrication of IDPMAP and iontophoresis-driven device

An iontophoresis-driven porous MA drug delivery system, including IDPMAP and iontophoresis-driven device, was developed for active transdermal drug delivery, as shown in Figure 2a and Figure S2. The PCB and its detailed schematic circuit diagram of iontophoresis-driven device are shown in Figure 2b and Figure S3, respectively. Iontophoresis-driven circuit mainly consists of three modules: power supply circuit, micro control unit (MCU) and voltage-controlled constant current circuit. The power of iontophoresis device can be supplied by USB port or lithium battery. USB port can directly power the iontophoresis-driven device or charge lithium battery. Full-charged lithium battery also can directly provide power for the iontophoresis-driven device. Low energy chip of MSP430F169 integrated with D/A converter was chosen as the MCU of iontophoresis-driven device. According to the input modes (current magnitude, duty cycle and frequency), MCU was programmed to output PWM voltage waves via D/A converter. A voltage-controlled constant current circuit was proposed to maintain a constant iontophoresis current through the skin. The iontophoresis current amplitude can be tuned by PWM

Electronic copy available at: https://ssrn.com/abstract=3677349

voltage of MCU. Once the iontophoresis current is applied on the IDPMAP, the liquid drug capsuled in charged nanovesicles can be actively delivered into systemic circulation. The iontophoresis-driven device is portable for self-administration with a small size of 44× 38 ×10 mm^3 and a light weight of only 21 g.

The assembled IDPMAP with a diameter of 34 mm is shown in Figure 2a&c. IDPMAP mainly consists of a porous MA, an anti-seepage gasket, a conductive hydrogel, and two Ag/AgCl electrodes on flexible PCB. Porous MA has many randomly distributed pores for liquid drug storage and delivery. The anti-seepage gasket effectively insulates two electrodes to avoid current short circuit and prevent liquid drug leakage. The gasket made from adhesive tape can closely stick IDPMAP on the patient skin. The conductive gel is designed to enhance the conductivity between Ag/AgCl electrode and skin. The electrodes on flexible PCB are connected with the output current ports of iontophoresis-driven device. The iontophoresis-driven current can be applied on porous MA loaded with nanovesicle solution and conductive gel via two electrodes.

Diabetes is one of the most serious chronic diseases with a rapid increasing number of patients [31]. Insulin is one of the most effective drugs to tune BGL for type 1 and advanced type 2 diabetic patients [31, 43]. Moreover, it has been demonstrated that iontophoresis with charged insulin nanovesicles can effectively promote transdermal insulin delivery [18]. Herein, we prepared charged insulin nanovesicles for diabetes treatment, as shown in Figure 2d-f. Insulin nanovesicles are in spherical shape with a defined edge. The average diameter and potential of nanovesicles were 200 nm and positive 13.8 mV, respectively. The nanovesicles acted as the effective carrier of insulin and permeation enhancer. Insulin is encapsulated in nanovesicles with high entrapment efficiency, which can avoid the charge reversal of insulin iontophoresis through the skin [18, 44]. The prepared insulin nanovesicles were dripped in the porous MA of IDPMAP.

Porous MA is the key componet of IDPMAP and its morphology is shown in Figure 2g-i. The porous MA is in milky white. Porous MA consists of 138 conical microneedles, which are concentrically and uniformly arranged on the substrate. The average height, tip diameter, and base diameter of conical microneedles are approximately 800 μm, 30 μm, and 400 μm, respectively. Numerous randomly distributed micro-pores with a variety of pore sizes (hundreds of nanometers up to several micrometers) could be clearly observed in the microneedle (Figure 2j). The porosity of porous MA is measured at approximately 43 % according to the method previously reported [27]. The blue ink stored in a sponge was rapidly absorbed into porous MA and transferred toward a paper through microneedle tips by capillary action, as shown in Figure S5 and Video S2. It well demonstrated that porous MA has enough inter-connective micro-channels for liquid drug storage and capillary transport. Moreover, a modified IDPMAP was designed to further improve its storage capacity of liquid drugs, as shown in Figure S6.

Electronic copy available at: https://ssrn.com/abstract=3677349

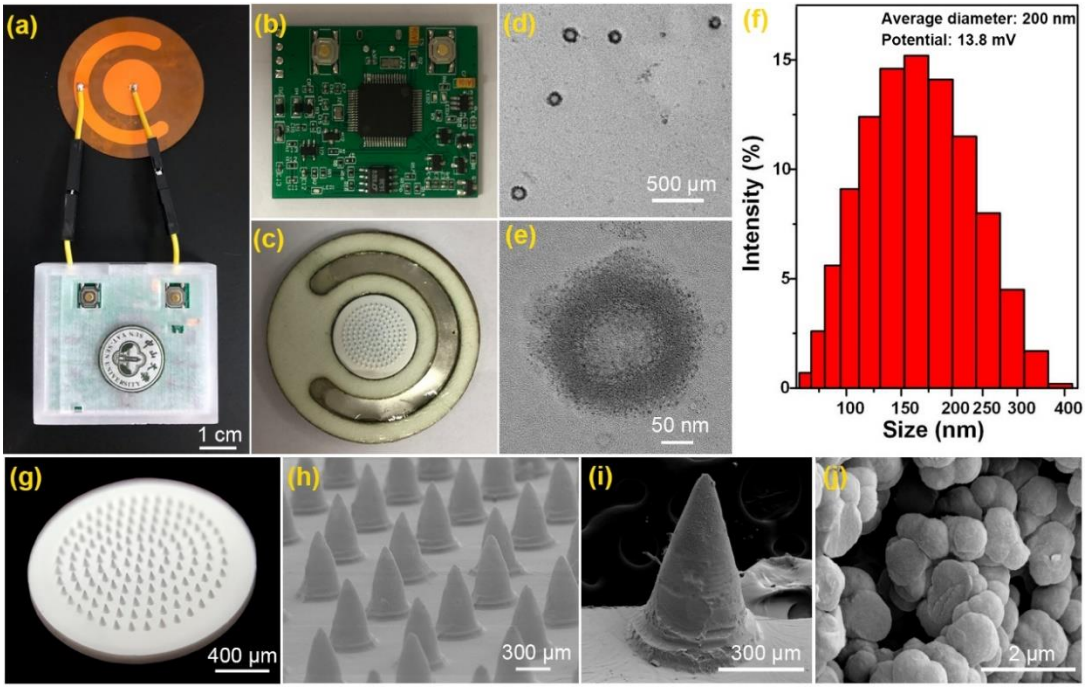

Figure 2 (a) The iontophoresis-driven porous MA drug delivery system. (b) PCB of iontophoresis-driven device. (c) IDPMAP for transdermal drug delivery. (d-e) TEM images of insulin nanovesicles. (f) Size distribution of insulin nanovesicles. (g) Optical image of porous MA. Porous MA is in milky white. (h) SEM image of porous MA. (i) SEM image of one porous microneedle. The tip is sharp. (j) SEM image of porous microneedle surface. The micro-pores could be clearly observed.

3.3 Mechanical performance of IDPMAP

Porous MA of IDPMAP should penetrate in the skin without breakage for facilitating liquid drug delivery, thus the mechanical performance of IDPMAP was investigated, as shown in Figure 3. The fracture performance of IDPMAP was tested, as shown in Figure 3a. The resistance force increased with the loading displacement till at point "P" , where exsited a sudden drop due to the microneedle breakage at tips (fracture microneedle shown in Figure 3a, insert). The fracture force per microneedle of IDPMAP was approximately 134 mN/needle. The penetration performance of IDPMAP was also measured, as shown in Figure 3b. The insertion force acted on the rabbit skin by porous MA increased with the loading displacement until it was beyond the rupture limit of rabbit skin, resulting in rapid skin penetration at point "Q", where appeared a rapid drop [45]. Thus, the skin penetration force per microneedle of IDPMAP was 17.8 mN/needle, which is much lower than fracture force per microneedle. It indicates that porous MA of IDPMAP can realize successful skin penetration without breakage, which was further demonstrated by punctured rabbit skin (Figure 3b, insert) and intact porous microneedle (Figure 3b, insert) after skin penetration test.

Figure 3c shows the rabbit skin punctured by IDPMAP loaded with red tissue-marking dye in the microneedle tips. It could be clearly observed that neatly arranged microhole array was left on the rabbit skin, whose distribution fitted well with the arrangement of porous MA. The successful skin penetration rate was more than 99 %. The punctured rabbit skin was further observed by OCT, as shown in Figure 3d. The rabbit skin was sucessfully penetrated by IDPMAP. The average depth of microhole array in the skin was approximately 400 μm, suggesting that IDPMAP could effectively penetrate throught 10-20 μm

Electronic copy available at: https://ssrn.com/abstract=3677349

stratum corneum layer of skin for transdermal drug delivery. In general, IDPMAP exhibits good mechanical strength for skin penetration.

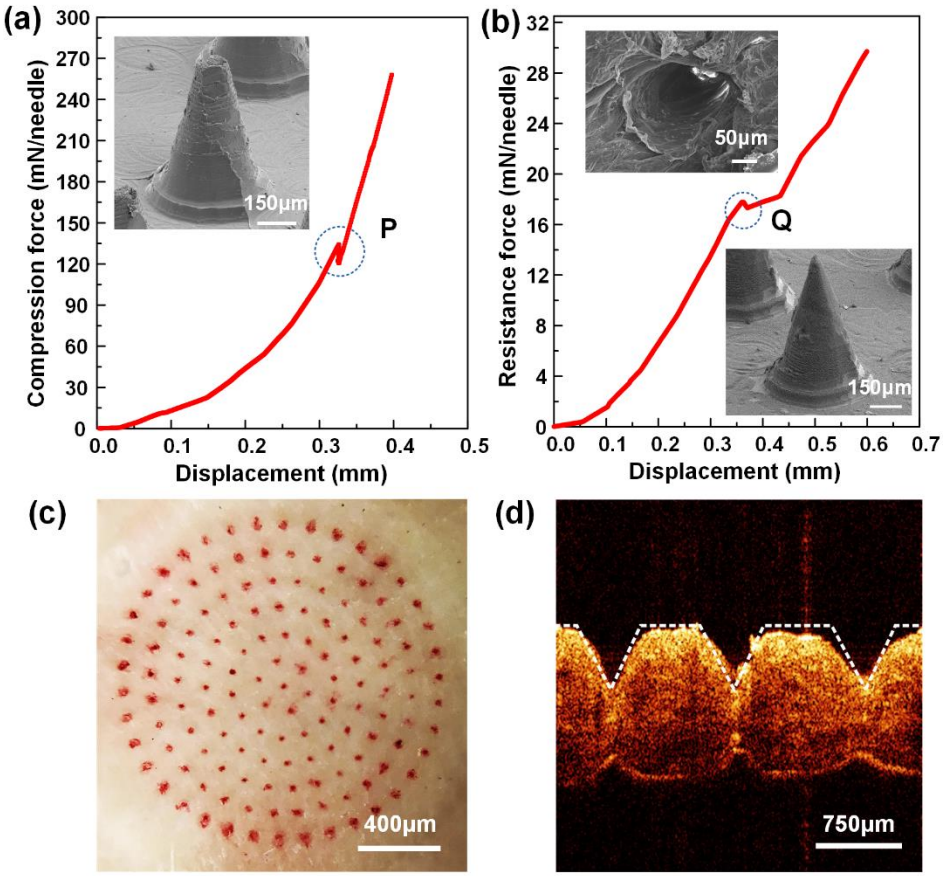

Figure 3 (a) The relationship of loading force and displacement during IDPMAP fracture test. The fracture force per microneedle was approximately 134 mN/needle. The insert: SEM image of a broken microneedle after fracture test. (b) The relationship of resistance force and loading displacement during IDPMAP penetration test. The penetration force per microneedle was approximately 17.8 mN/needle. The inserts: the SEM images of punctured rabbit skin and microneedle after penetration test, respectively. (c) Representative bright-field image of rabbit skin punctured by IDPMAP loaded with red tissue-marking dye in the microneedle tips. (d) OCT image of the rabbit skin punctured by IDPMAP. It indicates that porous MA sucessfully penetrated in the rabbit skin.

3.4 Biocompatibility of IDPMAP

The anti-seepage gasket and conductive hydrogel of IDPMAP are correspondingly made from medical tape and agarose hydrogel with normal saline, which have been demonstrated good biocompatibility [46]. The porous MA, the key part of IDPMAP, directly penetrates in the skin for liquid drug delivery, whose biocompatibility should be further investigated. To evaluate the cytotoxicity of porous MA, NIH/3T3 fibroblasts were incubated with the released media of porous MA and the cell viability was measured by MTT assay (Figure 4a). The cell activity of group treated by porous MA shows no significant difference with that of control group. It indicates that porous MA has little adverse effect on cell growth and proliferation. To evalute the lethality of porous MA against cells, a Calcein-AM/PI kit was employed to stain the cells co-incubated with the release media for 48 h. Figure 4b presents fluorescence microscope images of NIH/3T3 cells stained by Live/Dead assay, where living cells are in

Electronic copy available at: https://ssrn.com/abstract=3677349

green fluorescence and dead cells are in red fluorescence. No obvious increase of dead cells was observed in comparison with that in control group, suggesting that the porous MA has good biocompatibility.

To further assess the skin recovery ability, SD rats was treated by IDPMAP loaded with PBS solution with 1 mA iontophoresis on the dorsum without hair for 12 h. The images of skin recovery process after removal of IDPMAP are shown in Figure 4c. The microhole array on the skin punctured by porous MA was completely healed within an hour without obvious erythema and lesions. To further evaluate the possibility of inflammatory cells, diabetic rats were firstly treated by IDPMAP with 1 mA iontophoresis for 12 h. After removal of IDPMAP from SD rats for 24 h, the cross sections of skin tissues were cut and stained with hematoxylin and eosin (H&E). The histological images of H&E-stained skin tissues are shown in Figure 4d, no significant increase of inflammatory cells were observed in the skin treated by IDPMAP with 1 mA iontophoresis in comparison with untreated skin. Thus, IDPMAP with iontophoresis may not trigger an inflammatory response. Above all, IDPMAP is a biocompatible device for transdermal drug delivery.

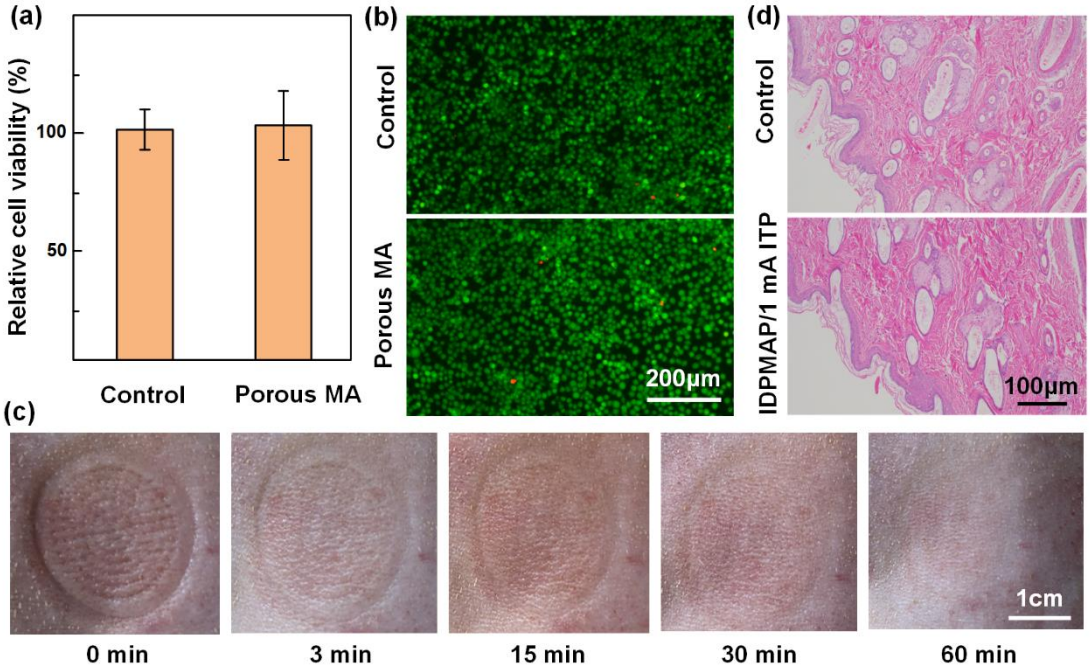

Figure 4 (a) NIH/3T3 fibroblasts were incubated with the released media of porous MA for 48 h and the cell viability was detected by MTT assay. Error bars indicate SD (n = 6). (b) Fluorescence microscope images of NIH/3T3 cells stained by Live/Dead assay, in which living and dead cells are in green and red fluorescence, respectively. (c) The skin recovery process after 12 h treatment using IDPMAP with 1 mA iontophoresis. The treated skin could self-recover in 1 h. (d) Representative H&E-stained skin sections administrated using IDPMAP with 1 mA iontophoresis. IDPMAP with iontophoresis triggered no inflammatory response.

3.5 *In vivo* transdermal insulin delivery in diabetic rats

The effect of iontophoresis and porous MA of IDPMAP on *in vitro* transdermal permeation performance was analyzed, as shown in Figure S7&8. Negatively charged Calcein was selected as a model drug for *in vitro* permeation tests [20]. The Calcein cumulative permeation amounts of each group were measured, as shown in Figure S9a. The cumulative amount of Calcein increased with administration

Electronic copy available at: https://ssrn.com/abstract=3677349

period. A significant difference of cumulative permeation amount can be observed among these groups after 5 h treatment, as shown in Figure S9b. The combination of IDPMAP with iontophoresis showed the best Calcein release performance. Iontophoresis promoted the transdermal Calcein delivery attributed to electromigration [20]. The Calcein stored in porous MA of IDPMAP can passively and effectively diffused into skin via interconnecting pores according to the Fick's Law.

Insulin therapy is one of the most effective treatment for type 1 diabetes with insulin deficiency and type 2 diabetes with impaired islet β-cell function. *In vivo* transdermal insulin nanovesicles thereby using an IDPMAP on a type 1 diabetic rat is shown in Figure 5a and Video S3. This insulin nanovesicles delivery was actively driven by an iontophoresis-drive device. BGLs of diabetic rats administrated with 5 IU insulin nanovesicles using different transdermal delivery approaches are shown in Figure 5b. The BGL of rats between 200 mg/dl and 100 mg/dl is defined as the normoglycemic state [47]. The BGLs of healthy group and control group presented negligible fluctuation and were stable at 108.2 ± 4.7 mg/dL and 408.1 ± 18.7 mg/dL, respectively. The BGLs of IDPMAP/1 mA ITP group decreased gently from initial hyperglycemic state of 438.6 ± 25.5 mg/dL to the normoglycemic state of 153.6 ± 18.4 mg/dL within 3 h and lasted the normoglycemic state for more than 5.5 h without hypoglycemia. However, as for the subcutaneous injection group, the BGLs declined rapidly from 441.6 ± 38.2 mg/dL to 218.4 ± 19.1 mg/dl within 1 h and to 55.8 ±15.3 mg/dL in next 2 h, which exceeded the normal range of blood glucose and had a risk of hypoglycemia [32, 48]. And the BGLs rapidly rebounded to original hyperglycemic state within 4 h. Therefore, the subcutaneous injection of 5 IU insulin nanovesicles exhibited strong hypoglycemic effect but may induce a risk of hypoglycemia. Subcutaneous injection is usually associated with pain, needle phobia, and the risk of infection, while IDPMAP is painless and may effectively lower cross contamination.

The average normoglycemic periods of each group treated by different delivery approaches are shown in Figure 5c. The average normoglycemic periods of subcutaneous injection group, IDPMAP/0 mA ITP group, IDPMAP/0.5 mA ITP group, IDPMAP/1 mA ITP (1:1) group, and IDPMAP/1 mA ITP group were approximately 2 h, 3.5 h, 4.5 h, 4.9 h, and 5.4 h, respectively. IDPMAP/1 mA ITP group exhibited the best hypoglycemic effect on the type 1 diabetic rats. The combination of drug diffusion and iontophoresis across inter-connecting pores into skin may lead to a synergistic enhancement in transdermal delivery rate of therapeutic insulin nanovesicles. The average normoglycemic period of IDPMAP/1 mA ITP group is approximately 2.7-fold of that of subcutaneous injection group, indicating porous MA combined with iontophoresis effectively promote *in vivo* delivery of the positively charged insulin nanovesicles. The average normoglycemic periods of IDPMAP/0 mA ITP group, IDPMAP/0.5 mA ITP group, and IDPMAP/1 mA ITP group are almost linearly increased with iontophoresis current. The mild iontophoresis current can drive charged insulin nanovesicles through micro-holes of porous MA into systemic circulation by the predominant driving forces of electromigration and electroosmosis [37-39]. The amount of transported therapeutic insulin nanovesicles could be actively controlled by applied iontophoresis current [21, 40, 41]. The average normoglycemic periods of IDPMAP/1 mA ITP (1:1) was 0.4 h longer than that of IDPMAP/0.5 mA ITP. It may be explained that the pulse current may reduce the polarization of the skin.

Electronic copy available at: https://ssrn.com/abstract=3677349

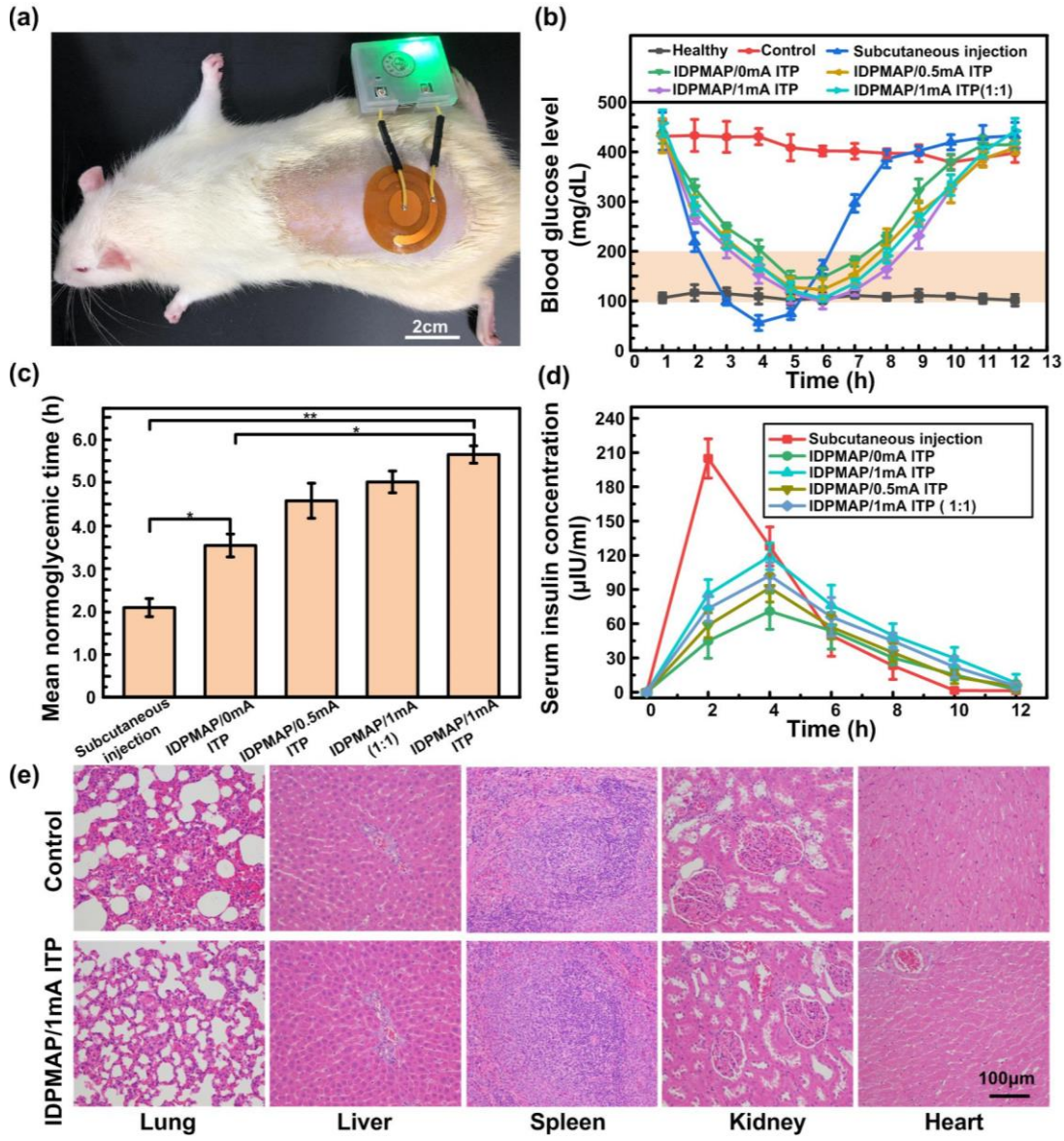

Figure 5 (a) The iontophoresis-driven porous MA drug delivery system for *in vivo* treatment of a diabetic rat. IDPMAP loaded with 5 IU insulin nanovesicles was attached on a rat skin with hair shaved. (b) The BGLs of STZ-induced type-1 diabetic rats administrated with 5 IU insulin nanovesicles using different transdermal delivery approaches. (c) The mean normoglycemic time of each group. (d) The serum insulin concentration of diabetic rats after application of IDPMAPs or subcutaneous injection of 5 IU insulin nanovesicles. (e) Hematoxylin and eosin staining of main organs (lung, liver, spleen, kidney and heart) in IDPMAP/1mA ITP group and control group.

The serum insulin levels of diabetic rats treated by different transdermal delivery approaches were further measured to determine the relative bioavailability of delivered insulin. Figure 5d presents the serum insulin levels of diabetic rats treated by IDPMAPs and subcutaneous injection. The serum insulin levels of rats treated by IDPMAPs and subcutaneous injection showed the similar tendency, which was mutually verified by the corresponding BGLs shown in Figure 5b. According to Figure 5d, the pharmacokinetic parameters of serum insulin levels were calculated [48], as listed in Table 2. Area under curve (AUC) is the total area under the curve of serum insulin level treated by IDPMAPs and subcutaneous injection. Bioavailability (BA) is equal to the AUC of each group divided by AUC of

Electronic copy available at: https://ssrn.com/abstract=3677349

subcutaneous injection group. C_{max} is the maximum serum insulin concentration at the treated period T_{max}. The serum insulin level of diabetic rats treated by subcutaneous injection reached its maximum value C_{max} of 204.87 μIU/ml at T_{max} of 2 h after administration, and its AUC was about 815.22 μIU·h/ml. Comparatively, T_{max} of IDPMAPs was 4 h, which was 2 h later than that of subcutaneous injection, owing to slowly passive diffusion and active iontophoresis of insulin nanovesicles from porous MA into the system circulation. C_{max} and BA of IDPMAP/1 mA ITP group were 119.09 μIU/ml and 89.4%, respectively. They were the highest among the IDPMAP groups, implying that the insulin nanovesicles stored in IDPMAPs may not be completely released into the system circulation and the iontophoresis provided an external driving force to promote the delivery of positively charged insulin nanovesicles. The BA and C_{max} of IDPMAP/0.5 mA ITP group were lower than those of IDPMAP /1mA ITP (1:1) group, indicating that pulse iontophoresis current may eliminate polarization and facilitate the delivery of insulin nanovesicles driven by iontophoresis. Above all, according to the *in vitro* and *in vivo* transdermal drug delivery tests, IDPMAP combined with iontophoresis provides a valuable alternative for effective and long-lasting transdermal delivery of charged liquid drugs.

Table 2 Pharmacokinetic parameters of each group

Group name	T_{max} (h)	C_{max} (μIU/ml)	AUC (μIU·h/ml)	BA (%)
Subcutaneous injection	2	204.87 ±17.21	815.22 ±77.85	100.00
IDPMAP/0 mA ITP	4	70.95 ±15.87	432.27 ±43.87	53.0
IDPMAP/1 mA ITP	4	119.09 ±11.71	728.85 ±30.02	89.4
IDPMAP/0.5 mA ITP	4	91.49 ±12.42	515.55 ±29.36	63.2
IDPMAP/1 mA ITP (1:1)	4	102.19 ±11.65	622.40 ±25.42	76.3

The possible effect of *in vivo* treatment with IDPMAP and iontophoresis on the safety of diabetic rats was investigated. The slices of lung, liver, spleen, kidney and heart of diabetic rats administrated with IDPMAP/1mA ITP group were observed by comparing with those of control group, as shown in Figure 5e. The morphologies of lung, liver, spleen, kidney and heart of diabetic rats treated by IDPMAP with 1mA iontophoresis were similar to those of control group. There were no abnormal changes and inflammatory reaction in lung, liver, spleen, kidney and heart in IDPMAP/1mA ITP group. Therefore, these finds may support that IDPMAP with iontophoresis is safe for the receptors, which may substantially improve patient tolerability and treatment outcomes.

4. CONCLUSION

We developed a novel IDPMAP and its matching portable iontophoresis-driven device for actively transdermal delivery of charged liquid drugs. IDPMAP integrated the technologies of porous MA, iontophoresis and charged nanovesicles, whose drug administration strategy was a combination of passive diffusion and active iontophoresis of charged nanovesicles capsuled with liquid drug. Charged nanovesicles stored in porous MA was diffused and iontophoresis driven into system circulation via interconnecting pores of porous MA. IDPMAP exhibited excellent skin penetration ability and good biocompatibility without skin irritation and hypersensitivity. *In vitro* transdermal permeation of negatively charged Calcein test and *in vivo* transdermal insulin nanovesicles delivery in diabetic rats demonstrated that the IDPMAP coupled iontophoresis could effectively regulate BGLs, maintain normoglycemia, and avoid the critical risk of hypoglycemia. Moreover, IDPMAP with mild

Electronic copy available at: https://ssrn.com/abstract=3677349

iontophoresis current raised no safety concern. Above all, IDPMAP combined with iontophoresis offers a platform technique for effective delivery of charged liquid drugs in an active-controlled manner.

Data Availability

All data generated or analyzed during this study are included in the published article and its Supplementary Information, and are available from the corresponding author on reasonable request.

Acknowledgements

This research is financially supported by the National Natural Science Foundation of China (Project No. 51975597), the Natural Science Foundation of Guangdong Province (Project No. 2019A1515011011), the General Program of Shenzhen Innovation Funding (Project No. JCYJ20170818164246179), the Special Support Plan for High Level Talents in Guangdong Province (Project No. 2017TQ04X674), and the Fundamental Research Funds for the Central Universities (No. 20lgzd27).

Conflicts of interest

The authors declare no conflict of interest.

References

[1] M.R. Prausnitz, S. Mitragotri, R. Langer, Current status and future potential of transdermal drug delivery, Nat Rev Drug Discov 3(2) (2004) 115-24.

[2] A.C. Anselmo, Y. Gokarn, S. Mitragotri, Non-invasive delivery strategies for biologics, Nat Rev Drug Discov 18(1) (2019) 19-40.

[3] M.R. Prausnitz, R. Langer, Transdermal drug delivery, Nat Biotechnol 26(11) (2008) 1261-8.

[4] H. Lee, C. Song, S. Baik, D. Kim, T. Hyeon, D.H. Kim, Device-assisted transdermal drug delivery, Adv Drug Deliv Rev 127 (2018) 35-45.

[5] K. van der Maaden, W. Jiskoot, J. Bouwstra, Microneedle technologies for (trans)dermal drug and vaccine delivery, J Control Release 161(2) (2012) 645-55.

[6] A.F. Moreira, C.F. Rodrigues, T.A. Jacinto, S.P. Miguel, E.C. Costa, I.J. Correia, Microneedle-based delivery devices for cancer therapy: A review, Pharmacol Res 148 (2019) 104438.

[7] X. Chen, L. Wang, H. Yu, C. Li, J. Feng, F. Haq, A. Khan, R.U. Khan, Preparation, properties and challenges of the microneedles-based insulin delivery system, J Control Release 288 (2018) 173-188.

[8] J. Yu, J. Wang, Y. Zhang, G. Chen, W. Mao, Y. Ye, A.R. Kahkoska, J.B. Buse, R. Langer, Z. Gu, Glucose-responsive insulin patch for the regulation of blood glucose in mice and minipigs, Nat Biomed Eng 4(5) (2020) 499-506.

[9] Y.H. An, J. Lee, D.U. Son, D.H. Kang, M.J. Park, K.W. Cho, S. Kim, S.H. Kim, J. Ko, M.H. Jang, J.Y. Lee, D.H. Kim, N.S. Hwang, Facilitated Transdermal Drug Delivery Using Nanocarriers-Embedded Electroconductive Hydrogel Coupled with Reverse Electrodialysis-Driven Iontophoresis, ACS Nano 14(4) (2020) 4523-4535.

[10] E. Larrañeta, R.E.M. Lutton, A.D. Woolfson, R.F. Donnelly, Microneedle arrays as transdermal and intradermal drug delivery systems: Materials science, manufacture and commercial development, Materials Science and Engineering: R: Reports 104 (2016) 1-32.

[11] Y. He, C. Hong, J. Li, M.T. Howard, Y. Li, M.E. Turvey, D. Uppu, J.R. Martin, K. Zhang, D.J. Irvine, P.T. Hammond, Synthetic Charge-Invertible Polymer for Rapid and Complete Implantation of Layer-by-

Electronic copy available at: https://ssrn.com/abstract=3677349

Layer Microneedle Drug Films for Enhanced Transdermal Vaccination, ACS Nano 12(10) (2018) 10272-10280.

[12] H.T.T. Duong, Y. Yin, T. Thambi, T.L. Nguyen, V.H. Giang Phan, M.S. Lee, J.E. Lee, J. Kim, J.H. Jeong, D.S. Lee, Smart vaccine delivery based on microneedle arrays decorated with ultra-pH-responsive copolymers for cancer immunotherapy, Biomaterials 185 (2018) 13-24.

[13] S.F. Taveira, A. Nomizo, R.F.V. Lopez, Effect of the iontophoresis of a chitosan gel on doxorubicin skin penetration and cytotoxicity, Journal of Controlled Release 134(1) (2009) 35-40.

[14] P.G. Green, Iontophoretic delivery of peptide drugs, Journal of Controlled Release 41(33-48) (1996).

[15] X.M. Wu, H. Todo, K. Sugibayashi, Enhancement of skin permeation of high molecular compounds by a combination of microneedle pretreatment and iontophoresis, J Control Release 118(2) (2007) 189-95.

[16] J.D. Byrne, M.R. Jajja, A.T. O'Neill, L.R. Bickford, A.W. Keeler, N. Hyder, K. Wagner, A. Deal, R.E. Little, R.A. Moffitt, C. Stack, M. Nelson, C.R. Brooks, W. Lee, J.C. Luft, M.E. Napier, D. Darr, C.K. Anders, R. Stack, J.E. Tepper, A.Z. Wang, W.C. Zamboni, J.J. Yeh, J.M. DeSimone, Local iontophoretic administration of cytotoxic therapies to solid tumors, Sci Transl Med 7(273 273ra14) (2015).

[17] T. Fukuta, Y. Oshima, K. Michiue, D. Tanaka, K. Kogure, Non-invasive delivery of biological macromolecular drugs into the skin by iontophoresis and its application to psoriasis treatment, J Control Release 323 (2020) 323-332.

[18] H. Chen, H. Zhu, J. Zheng, D. Mou, J. Wan, J. Zhang, T. Shi, Y. Zhao, H. Xu, X. Yang, Iontophoresis-driven penetration of nanovesicles through microneedle-induced skin microchannels for enhancing transdermal delivery of insulin, Journal of Controlled Release 139(1) (2009) 63-72.

[19] M.J. Garland, E. Caffarel-Salvador, K. Migalska, A.D. Woolfson, R.F. Donnelly, Dissolving polymeric microneedle arrays for electrically assisted transdermal drug delivery, J Control Release 159(1) (2012) 52-9.

[20] V. Kumar, A.K. Banga, Modulated iontophoretic delivery of small and large molecules through microchannels, International Journal of Pharmaceutics 434(1-2) (2012) 106-114.

[21] G. Qin, Y. Gao, Y. Wu, S. Zhang, Y. Qiu, F. Li, B. Xu, Simultaneous basal-bolus delivery of fast-acting insulin and its significance in diabetes management, Nanomedicine 8(2) (2012) 221-7.

[22] N.D. Singh, A.K. Banga, Controlled delivery of ropinirole hydrochloride through skin using modulated iontophoresis and microneedles, J Drug Target 21(4) (2013) 354-66.

[23] R.F. Donnelly, T.R. Singh, M.J. Garland, K. Migalska, R. Majithiya, C.M. McCrudden, P.L. Kole, T.M. Mahmood, H.O. McCarthy, A.D. Woolfson, Hydrogel-Forming Microneedle Arrays for Enhanced Transdermal Drug Delivery, Adv Funct Mater 22(23) (2012) 4879-4890.

[24] S. Katikaneni, A. Badkar, S. Nema, A.K. Banga, Molecular charge mediated transport of a 13 kD protein across microporated skin, Int J Pharm 378(1-2) (2009) 93-100.

[25] S. Yang, F. Wu, J. Liu, G. Fan, W. Welsh, H. Zhu, T. Jin, Phase-Transition Microneedle Patches for Efficient and Accurate Transdermal Delivery of Insulin, Advanced Functional Materials 25(29) (2015) 4633-4641.

[26] W. Luangveera, S. Jiruedee, W. Mama, M. Chiaranairungroj, A. Pimpin, T. Palaga, W. Srituravanich,

Electronic copy available at: https://ssrn.com/abstract=3677349

Fabrication and characterization of novel microneedles made of a polystyrene solution, J Mech Behav Biomed Mater 50 (2015) 77-81.

[27] L. Liu, H. Kai, K. Nagamine, Y. Ogawa, M. Nishizawa, Porous polymer microneedles with interconnecting microchannels for rapid fluid transport, RSC Advances 6(54) (2016) 48630-48635.

[28] J. Courtois, E. Byström, K. Irgum, Novel monolithic materials using poly(ethylene glycol) as porogen for protein separation, Polymer 47(8) (2006) 2603-2611.

[29] W. Li, R.N. Terry, J. Tang, M.R. Feng, S.P. Schwendeman, M.R. Prausnitz, Rapidly separable microneedle patch for the sustained release of a contraceptive, Nat Biomed Eng 3(3) (2019) 220-229.

[30] K. Chen, L. Ren, Z. Chen, C. Pan, W. Zhou, L. Jiang, Fabrication of Micro-Needle Electrodes for Bio-Signal Recording by a Magnetization-Induced Self-Assembly Method, Sensors (Basel) 16(9) (2016).

[31] S. Chen, H. Matsumoto, Y. Moro- oka, M. Tanaka, Y. Miyahara, T. Suganami, A. Matsumoto, Microneedle- Array Patch Fabricated with Enzyme- Free Polymeric Components Capable of On-Demand Insulin Delivery, Advanced Functional Materials (2018).

[32] Q.Y. Li, J.N. Zhang, B.Z. Chen, Q.L. Wang, X.D. Guo, A solid polymer microneedle patch pretreatment enhances the permeation of drug molecules into the skin, RSC Advances 7(25) (2017) 15408-15415.

[33] C. Wang, Y. Ye, G.M. Hochu, H. Sadeghifar, Z. Gu, Enhanced Cancer Immunotherapy by Microneedle Patch-Assisted Delivery of Anti-PD1 Antibody, Nano Lett 16(4) (2016) 2334-40.

[34] H.P. Tham, K. Xu, W.Q. Lim, H. Chen, M. Zheng, T.G.S. Thng, S.S. Venkatraman, C. Xu, Y. Zhao, Microneedle-Assisted Topical Delivery of Photodynamically Active Mesoporous Formulation for Combination Therapy of Deep-Seated Melanoma, ACS Nano 12(12) (2018) 11936-11948.

[35] Z. Luo, W. Sun, J. Fang, K. Lee, S. Li, Z. Gu, M.R. Dokmeci, A. Khademhosseini, Biodegradable Gelatin Methacryloyl Microneedles for Transdermal Drug Delivery, Adv Healthc Mater 8(3) (2019) e1801054.

[36] Z. Tong, J. Zhou, J. Zhong, Q. Tang, Z. Lei, H. Luo, P. Ma, X. Liu, Glucose- and H2O2-Responsive Polymeric Vesicles Integrated with Microneedle Patches for Glucose-Sensitive Transcutaneous Delivery of Insulin in Diabetic Rats, ACS Appl Mater Interfaces 10(23) (2018) 20014-20024.

[37] T.W. Wong, Electrical, magnetic, photomechanical and cavitational waves to overcome skin barrier for transdermal drug delivery, J Control Release 193 (2014) 257-69.

[38] P. Charoenputtakun, S.K. Li, T. Ngawhirunpat, Iontophoretic delivery of lipophilic and hydrophilic drugs from lipid nanoparticles across human skin, Int J Pharm 495(1) (2015) 318-328.

[39] S.-R. Kwon, S.H. Nam, C.Y. Park, S. Baek, J. Jang, X. Che, S.H. Kwak, Y.-R. Choi, N.-R. Park, J.-Y. Choi, Y. Lee, T.D. Chung, Electrodeless Reverse Electrodialysis Patches as an Ionic Power Source for Active Transdermal Drug Delivery, Advanced Functional Materials 28(15) (2018).

[40] H. Chen, H. Zhu, J. Zheng, D. Mou, J. Wan, J. Zhang, T. Shi, Y. Zhao, H. Xu, X. Yang, Iontophoresis-driven penetration of nanovesicles through microneedle-induced skin microchannels for enhancing transdermal delivery of insulin, J Control Release 139(1) (2009) 63-72.

[41] M.B. Delgado-Charro, R.H. Guy, Effective use of transdermal drug delivery in children, Adv Drug Deliv Rev 73 (2014) 63-82.

[42] R.R. Boinpally, S.L. Zhou, G. Devraj, P.K. Anne, S. Poondru, B.R. Jasti, Iontophoresis of lecithin

Electronic copy available at: https://ssrn.com/abstract=3677349

vesicles of cyclosporin A, Int J Pharm 274(1-2) (2004) 185-90.

[43] M.H. Ling, M.C. Chen, Dissolving polymer microneedle patches for rapid and efficient transdermal delivery of insulin to diabetic rats, Acta Biomater 9(11) (2013) 8952-61.

[44] K. Kajimoto, M. Yamamoto, M. Watanabe, K. Kigasawa, K. Kanamura, H. Harashima, K. Kogure, Noninvasive and persistent transfollicular drug delivery system using a combination of liposomes and iontophoresis, Int J Pharm 403(1-2) (2011) 57-65.

[45] J. Li, Y. Zhou, J. Yang, R. Ye, J. Gao, L. Ren, B. Liu, L. Liang, L. Jiang, Fabrication of gradient porous microneedle array by modified hot embossing for transdermal drug delivery, Mater Sci Eng C Mater Biol Appl 96 (2019) 576-582.

[46] J. Kim, I. Jeerapan, S. Imani, T.N. Cho, A. Bandodkar, S. Cinti, P.P. Mercier, J. Wang, Noninvasive Alcohol Monitoring Using a Wearable Tattoo-Based Iontophoretic-Biosensing System, ACS Sensors 1(8) (2016) 1011-1019.

[47] W. Yu, G. Jiang, D. Liu, L. Li, H. Chen, Y. Liu, Q. Huang, Z. Tong, J. Yao, X. Kong, Fabrication of biodegradable composite microneedles based on calcium sulfate and gelatin for transdermal delivery of insulin, Materials Science and Engineering: C 71 (2017) 725-734.

[48] S. Kim, H. Yang, J. Eum, Y. Ma, S. Fakhraei Lahiji, H. Jung, Implantable powder-carrying microneedles for transdermal delivery of high-dose insulin with enhanced activity, Biomaterials 232 (2020) 119733.

Electronic copy available at: https://ssrn.com/abstract=3677349

Click here to access/download;Figure(s);Figure 1C.tif

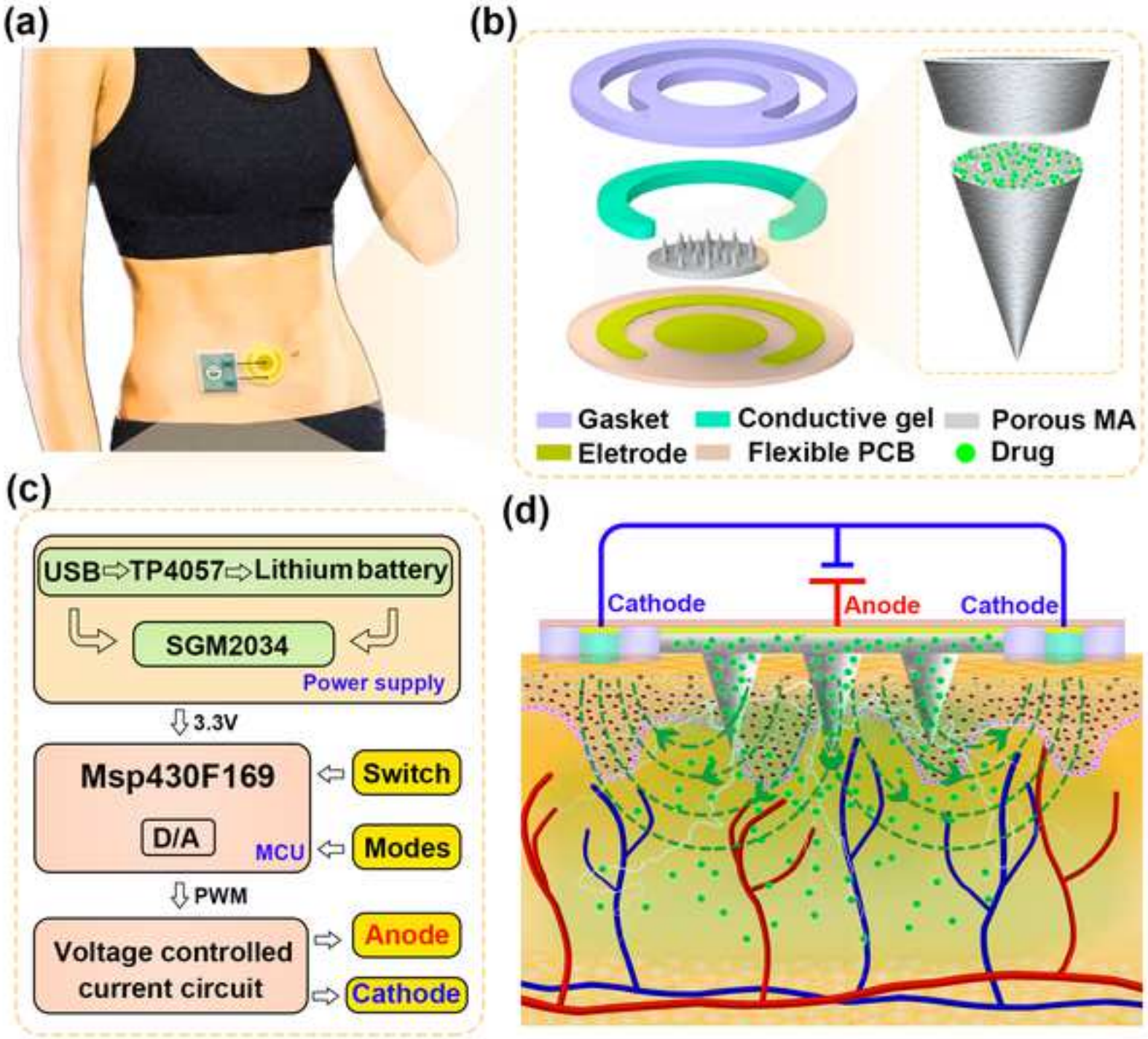

Electronic copy available at: https://ssrn.com/abstract=3677349

Click here to access/download;Figure(s);Figure 2C.tif

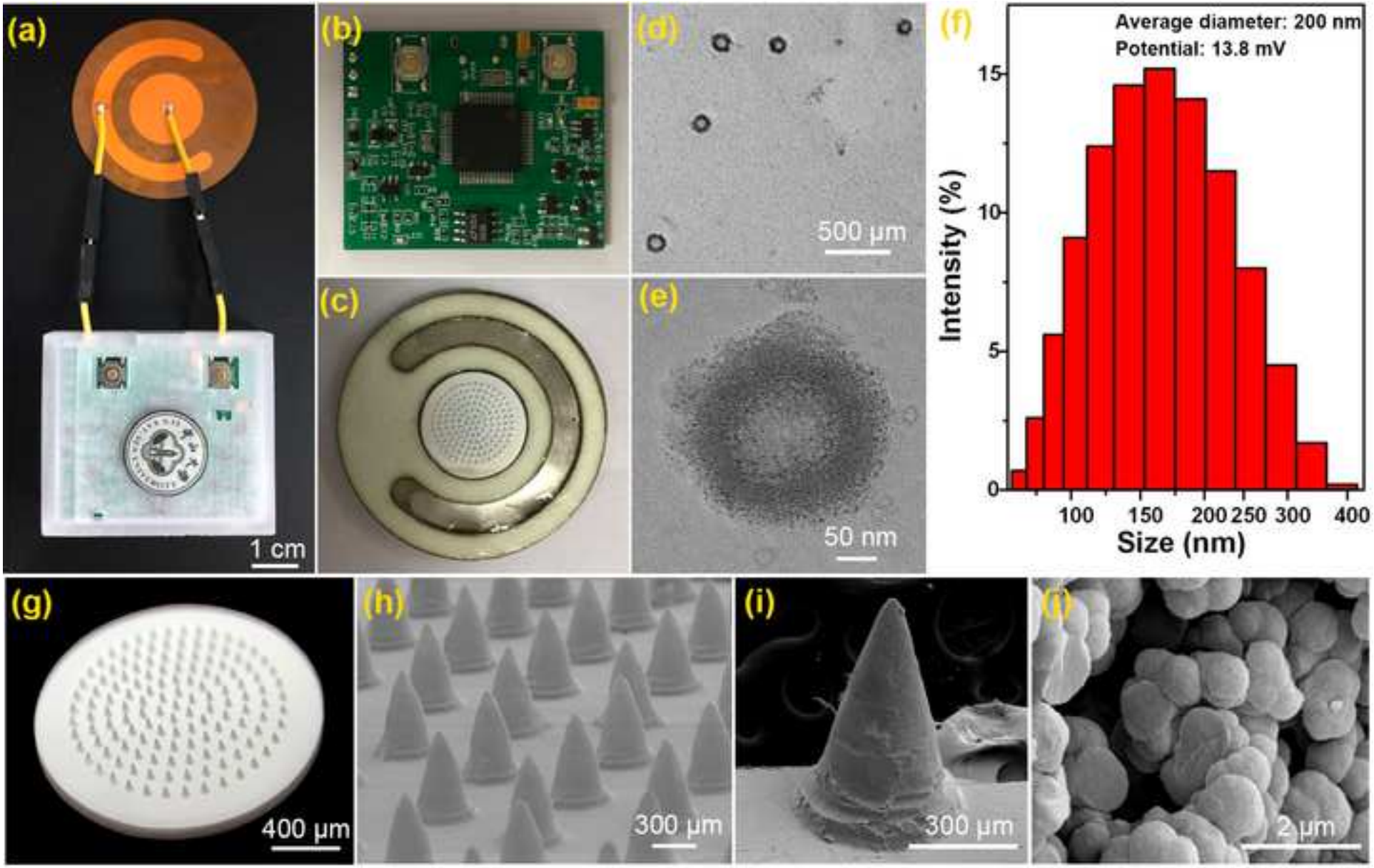

Electronic copy available at: https://ssrn.com/abstract=3677349

Click here to access/download;Figure(s);Figure 3C.tif

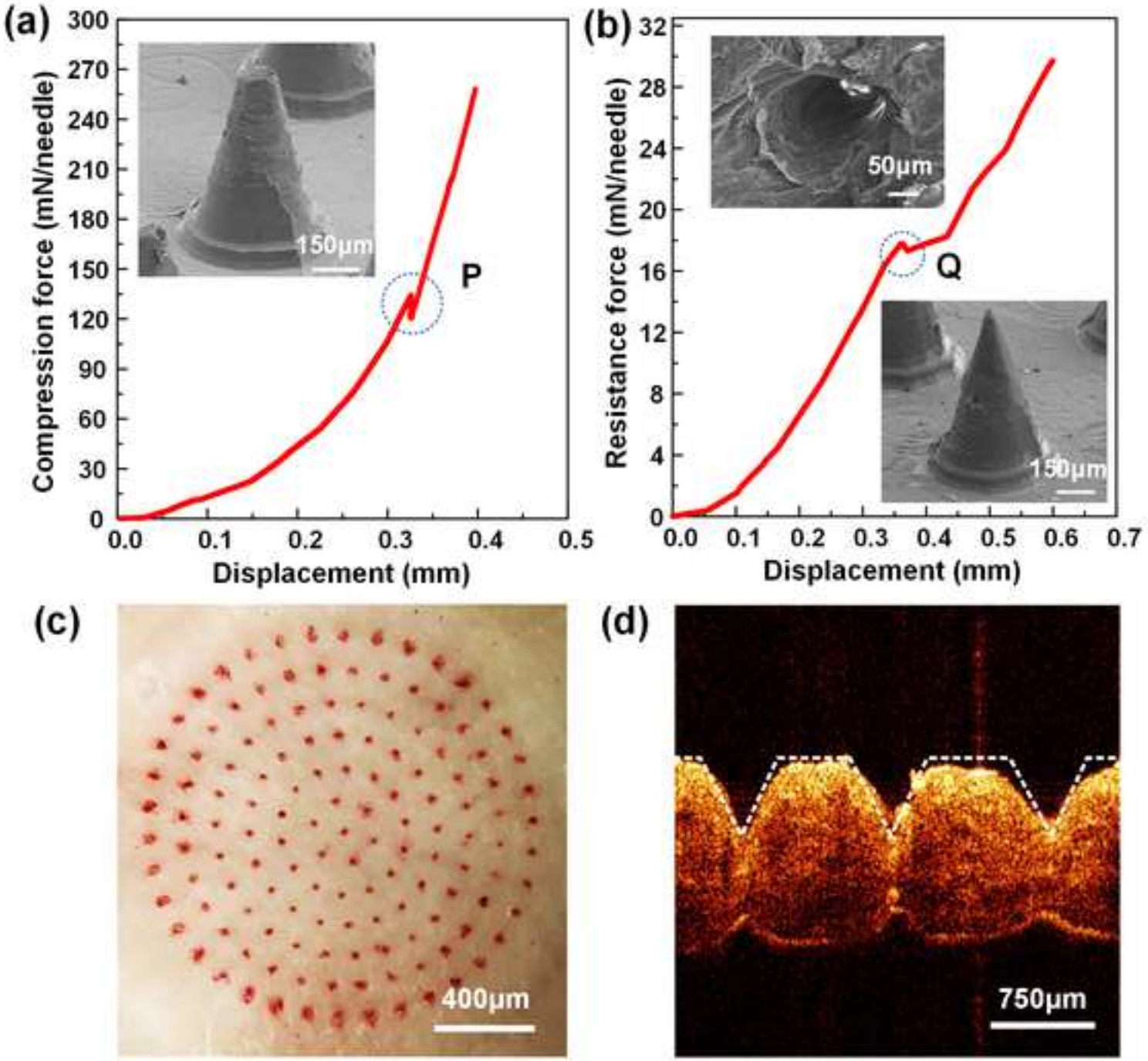

Electronic copy available at: https://ssrn.com/abstract=3677349

Click here to access/download;Figure(s);Figure 4C.tif

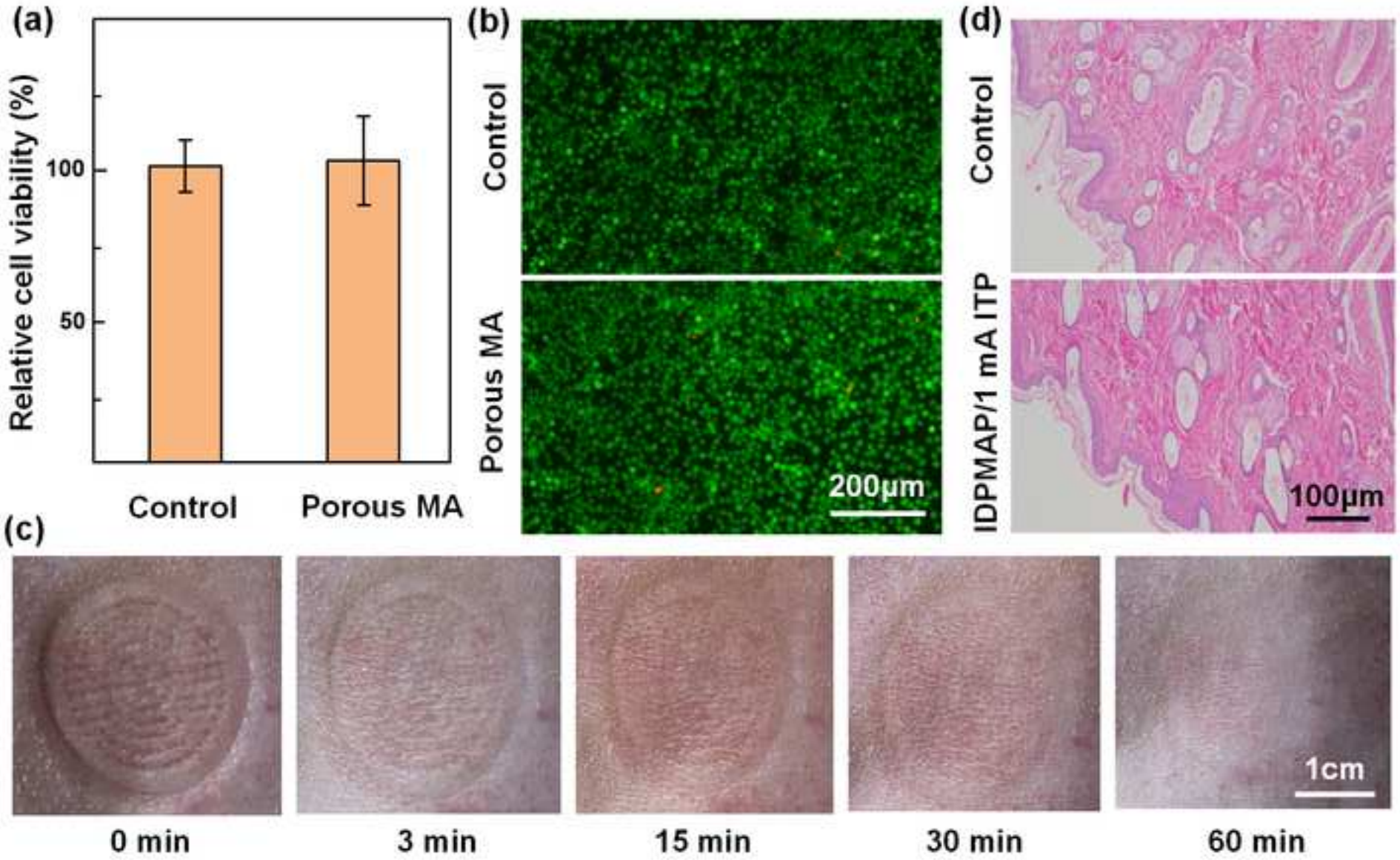

Electronic copy available at: https://ssrn.com/abstract=3677349

Click here to access/download;Figure(s);Figure 5.jpg

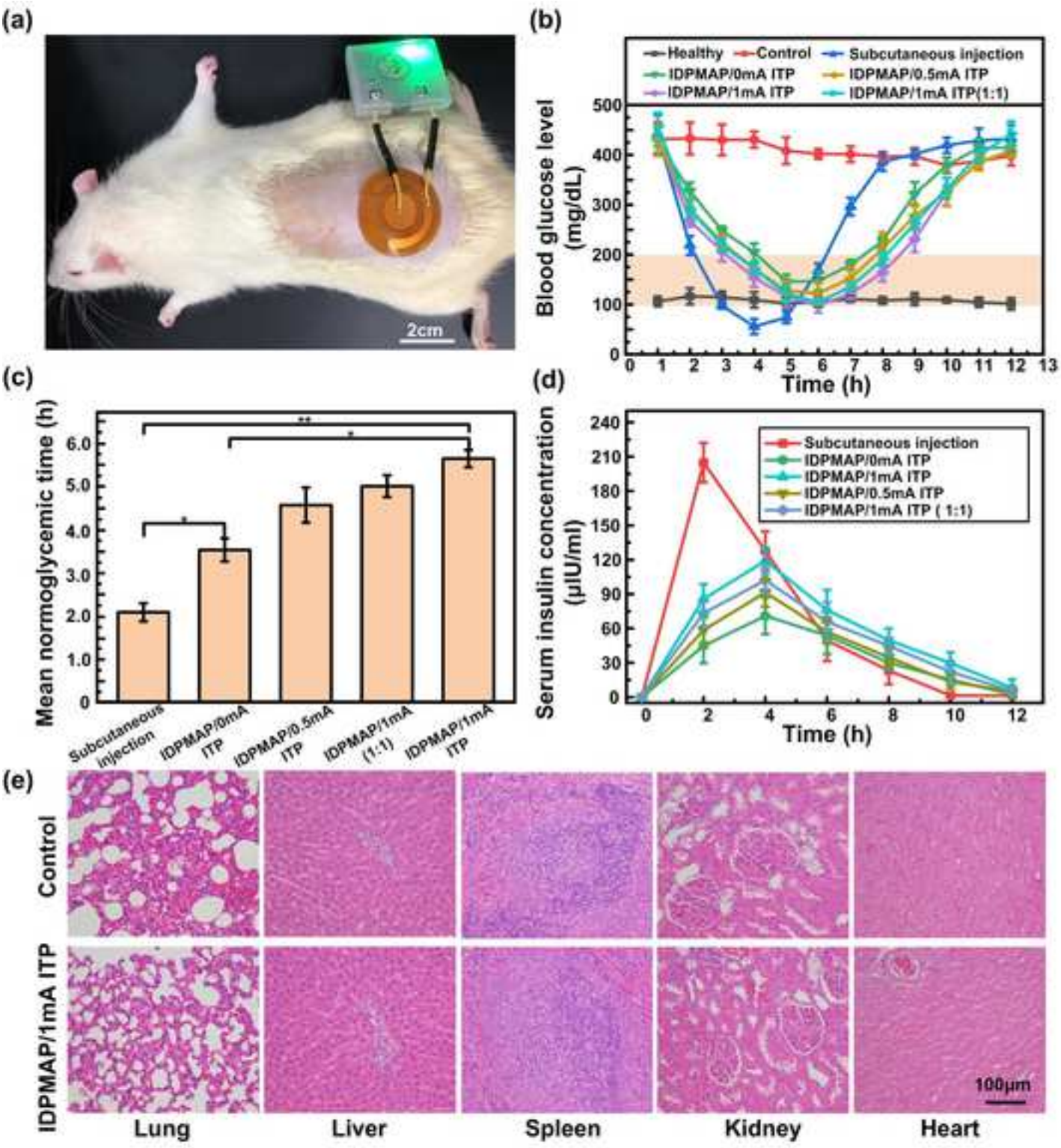

Electronic copy available at: https://ssrn.com/abstract=3677349

Figure(s1)

Click here to access/download
Supplementary Material
Figure S1C.tif

Electronic copy available at: https://ssrn.com/abstract=3677349

Figure(s2)

Click here to access/download
Supplementary Material
Figure S2.jpg

Electronic copy available at: https://ssrn.com/abstract=3677349

Figure(s3)

Click here to access/download
Supplementary Material
Figure S3.jpg

Electronic copy available at: https://ssrn.com/abstract=3677349

Figure(s4)

Click here to access/download
Supplementary Material
Figure S4C.tif

Electronic copy available at: https://ssrn.com/abstract=3677349

Figure(s5)

Click here to access/download
Supplementary Material
Figure S5C.tif

Electronic copy available at: https://ssrn.com/abstract=3677349

Figure(s6)

Click here to access/download
Supplementary Material
Figure S6C.tif

Electronic copy available at: https://ssrn.com/abstract=3677349

Figure(s7)

Click here to access/download
Supplementary Material
Figure S7C.tif

Electronic copy available at: https://ssrn.com/abstract=3677349

Figure(s8)

Click here to access/download
Supplementary Material
Figure S8C.tif

Electronic copy available at: https://ssrn.com/abstract=3677349

Figure(s9)

Click here to access/download
Supplementary Material
Figure S9.tif

Electronic copy available at: https://ssrn.com/abstract=3677349

Click here to access/download
Supplementary Material
Supporting information .docx

Electronic copy available at: https://ssrn.com/abstract=3677349

Click here to access/download
Supplementary Material
Video S1.mp4

Electronic copy available at: https://ssrn.com/abstract=3677349

Click here to access/download
Supplementary Material
Video S2.mp4

Electronic copy available at: https://ssrn.com/abstract=3677349

Click here to access/download
Supplementary Material
Video S3.mp4

Electronic copy available at: https://ssrn.com/abstract=3677349